Proceedings of ASME Turbo Expo 2020
Turbomachinery Technical Conference and Exposition
GT2020
September 21-25, Virtual, Online

GT2020-16084

NUMERICAL INVESTIGATION INTO THE IMPACT OF INJECTOR GEOMETRICAL DESIGN PARAMETERS ON HYDROGEN MICROMIX COMBUSTION CHARACTERISTICS

Xiaoxiao Sun*[1], Parash Agarwal[1], Francesco Carbonara[1], David. Abbott[1], Pierre. Gauthier[2], Bobby Sethi[1]

[1]School of Aerospace, Transport and Manufacturing, Cranfield University,
College Road, Cranfield, MK43 0AL, United Kingdom
[2]Siemens Canada Limited,
9545 Cote de Liesse Road, Montreal QC H9P 1A5, Canada

ABSTRACT

Hydrogen micromix combustion is a promising concept to reduce the environmental impact of both aero and land-based gas turbines by delivering carbon-free and ultra-low-NO_x combustion without the risk of autoignition or flashback. As a part of the ENABLEH2 project, the current study focuses on the influence of design parameters on the micromix hydrogen combustion injectors. This study provides deeper insights into the design space of a hydrogen micromix injection system via numerical simulations. The key geometrical design parameters of the micromix combustion system are the sizing of the air gates and the hydrogen injector orifices together with the offset distance between air gate and hydrogen injection, the mixing distance and the injector to injector spacing.

This paper first presents results of the numerical simulation of four designs, down selected from a series of combinations of the key design parameters, including cases with low and high momentum flux ratio, weak and strong flame-flame interaction. It was discovered that the hydrogen/air mixing characteristics, and flame to flame interactions, are the main factors influencing the combustor gas temperature distributions, flame lengths and the corresponding NOx production.

The current study then focused on the effect of air gate geometry on the mixing characteristics, flame shape and temperature distribution. The momentum flux ratio was kept constant throughout this investigation by keeping the air gate area constant. Variations of the original baseline air gate design were studied, followed by a study of various novel air gate geometries, including circular, semi-circular and elliptical shapes.

It is concluded that NOx production is influenced by a number of factors including jet penetration flame interactions and air gate shape and that there is a "Sweet Spot" that results in the lowest practicable NOx production. Flatter and wider air gate shapes tend to yield the lowest temperature and consequently the lowest NOx. Reduced interaction between flames also tends to reduce NOx and by manipulating hydrogen penetration, there is the potential to further reduce the NOx production.

Keywords: Hydrogen; Micromix; Combustion; Injector Design; Low emission

NOMENCLATURE

Abbreviations

AFR	Air to Fuel Ratio
CO_2	Carbon Dioxide
DOE	Design of Experiments
FGM	Flamelet Generated Manifold
H_2	Hydrogen
IRZ	Inner Recirculation Zone
JICF	Jet in Cross Flow
LHS	Lattice Hypercube Sampling
LH_2	Liquid Hydrogen
NOx	Nitrous Oxides
ORZ	Outer Recirculation Zone
OH	Hydroxyl Radical
PDF	Probability Density Function
RANS	Reynolds-Averaged Navier Stokes
SST	Shear Stress Transport

Symbols

c	mass fraction of fuel
J	Momentum Flux Ratio
S_n	Normalised Standard Deviation
u	Velocity
ϕ	Equivalence Ratio

* Address all correspondence to this author

ρ Density

INTRODUCTION

The increasing concern over global warming and other environmental issues leads to highly ambitious emissions targets being imposed on the civil aviation industry by legislation bodies. Flightpath 2050 targets a 75% reduction in CO_2 emission per passage kilometre, a 90% reduction in NOx emissions and a 65% reduction in perceived noise emission relative to year 2000 technologies by 2050 [1]. It has been reported in a number of projects [2, 3, 4] that these targets are unlikely to be met with carbon containing fuels, despite significant research efforts on advanced, disruptive airframe and propulsion technologies (including turbo/hybrid electric propulsion), even when coupled with improved asset and life cycle management procedures. Even if these targets could be met, this would not be sufficient in the longer term to give a fully sustainable future for civil aviation. In the meantime, it has been indicated that the growing consumption of aviation fuel will result in the aviation industry becoming "dirtier" by producing a higher proportion of the total amount of CO_2 emissions [5]. These, together with the depletion of fossil fuel resources make it necessary to develop clean and efficient technologies to allow sustainable growth in aviation.

Liquid hydrogen (LH2) has the potential to completely decarbonise civil aviation (both at mission and life cycle level) and significantly reduce the impact of aviation on the environment. Burning hydrogen will essentially generate zero mission level CO2, CO, UHC and PM, except for minimal contributions due to oil consumption. Hydrogen will give the much cleaner exhaust compared to hydrocarbon fuels and could contribute to reduced radiative forcing and thus to lower global temperature-rise from aviation. Since hydrogen has much wider stability limits than kerosene or methane, despite higher flame temperature at stoichiometric conditions, it is possible to employ leaner combustion with hydrogen in order to achieve ultra-low thermal NOx production. Moreover, the molecular diffusivity and high flame speed of hydrogen facilitates quicker mixing and lower residence time, reducing not only NOx production but also the combustor length. Also, the exceptionally high heat capacity of hydrogen provides a formidable heat sink, which can be used to produce engine concepts with much higher engine thermal efficiency and can facilitate the application of superconductivity in more advanced propulsion systems.

The ongoing H2020 ENABLEH2 project [6], coordinated by Cranfield University, aims to revitalise the enthusiasm in LH2 research for civil aviation and in doing so demonstrate that LH2 and related enabling technologies are a feasible and sustainable solution for long term, environmentally friendly civil aviation. The idea of LH2 being an aviation fuel has not been widely promoted within the industry, mainly due to the much higher cost associated with the on-board and land infrastructure required. However, it is expected that as time passes, humanity will realise that this higher price is worth paying given the environment benefits and the additional employment generated.

The concept of hydrogen Micromix combustion for aero engines was first studied Aachen University [7, 8], the concept utilises an array incorporating a large number of hydrogen flames at very lean conditions to limit flame temperature, hence the production of NOx. The concept is shown in Figure 1: hydrogen is injected via a circular orifice into accelerated air exiting the air gate, as jets in cross flow. This forms a non-premixed flame downstream reducing the risk of flashback and auto-ignition. The injectors are sufficiently small while the velocity of fuel and air are sufficiently high so that the flames are miniaturised but highly intensified to ensure improved mixing and very fast reaction compared to conventional lean burn injectors. The additional benefits of the micromix concept includes the control of fuel scheduling within the injector arrays at various engine operating conditions, which could potentially not only tailor the temperature distribution at combustor exit and reduce that near the liner, but also reduce, at an early stage, the chances of problems related to combustion thermoacoustics which often arises for lean combustion.

The research into hydrogen micromix combustion within the ENABLEH2 project is divided into three phases:

1. Small-scale injector down-selection and test
2. Full annular combustor segment performance assessment and emissions measurement
3. Sub-atmospheric altitude relight capability test.

The work presented in this paper is part of the Phase 1 of the project scope. The methodology for Phase 1 is shown in Figure 2. CFD simulations were performed to understand flow physics for the initial design and down-selection of the injectors, which will be tested at a range of test conditions with measurement of

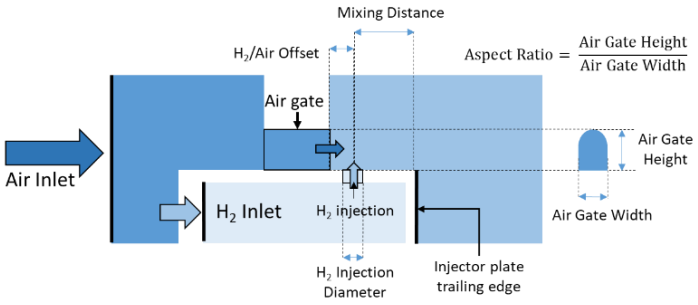

Figure 1. H_2 micromix single injector design parameters

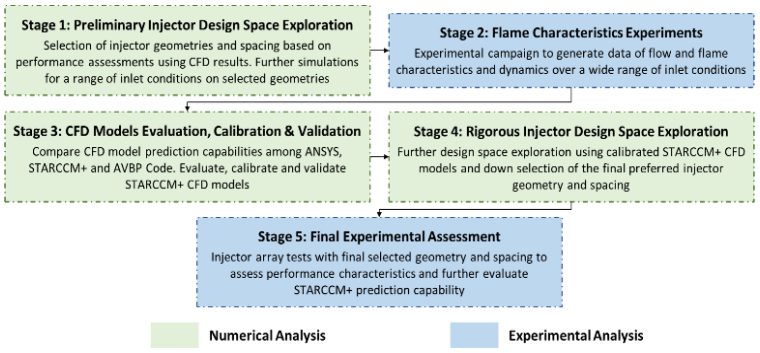

Figure 2. Numerical and experimental campaign methodology

flame, emissions and dynamics via laser imaging, gas analyser and pressure sensors. The generated test data will be used to evaluate, calibrate and validate numerical models. Various CFD codes are used, including ANSYS FLUENT and Star-CCM+ . With calibrated CFD model, more rigorous design space exploration will be carried out to determine the most promising design with regard to NOx emission and other performance characteristics. The final injector design will then be tested in an experimental rig, accompanied by high-fidelity CFD simulations.

In this paper, numerical simulations were conducted focusing on the effect of various geometrical design parameters. The first numerical study illustrates the difference in flow and flame characteristics of four down-selected geometries with different values of designs parameters. The impact of air gate geometry at constant momentum flux ratio in Sections 4 and 5 in which different flame shapes and temperature distributions were observed with vastly different NOx production. The detailed analysis on these effects provides evidence and useful guidance on achieving designs producing potentially ultra-low NOx.

1. Micromix injection geometrical design

Various geometrical parameters influence the design of a micromix combustion system, they are defined in Figure 1, including the air gate width, air gate height, the aspect ratio, hydrogen injection orifice diameter, air/hydrogen offset distance (i.e. the length between the air gate and hydrogen injection) and the mixing distance from hydrogen injection to the trailing edge of the injector plate. The vertical and horizontal spacing of the injectors are also defined as design parameters but are kept constant throughout the current study.

Each of these design parameters influences the shape, position and dynamics of the flames. For a jet in cross flow (JICF) the momentum flux ratio between the fuel jet and the air crossflow has a significant influence on fuel placement and thus flame characteristics. The momentum flux ratio is defined as:

$$J = \frac{\rho_j \times u_j^2}{\rho_\infty \times u_\infty^2} \qquad (1)$$

Where ρ_j represents the density of H_2, ρ_∞ represents the density of the free stream air and the u_j represents the H_2 flow velocity, u_∞ represents the velocity of the air at air gate exit. The momentum flux ratio between the two streams has a direct impact the penetration of H_2 into the air stream; the greater the momentum flux ratio, the greater is the penetration of the H_2 stream into the air stream; and hence the more distributed mixing in the vertical direction. The degree and the rate of the mixing process are important as they affect the combustion process. The combustion efficiency and the exhaust compositions are directly dependent upon the fuel/air mixture and the reaction kinetics. The chemical kinetics are difficult to control but, the mixing process is more readily controlled by varying the momentum flux ratio between the JICF streams.

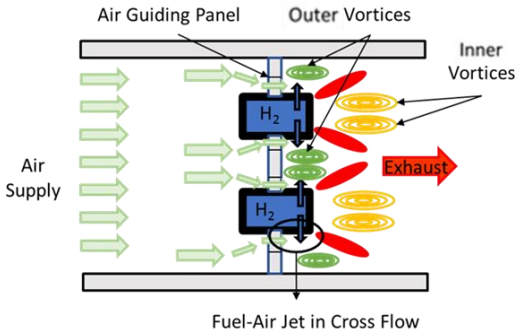

Figure 3: Schema of the typical hydrogen micromix flow field (adapted from [9])

As the airstream mixes with the penetrating H_2 stream, the mixing zone between the two streams is divided by the shear layer formed between them. Two distinct recirculation zones are formed, the inner recirculation zone (IRZ) and the outer recirculation zone (ORZ). The inner recirculation zone is formed by the recirculation of hot combustion products downstream of the H_2 penetration site and the outer zone is formed by the recirculation of the air downstream the air gate. Figure 3 depicts the formation of these two recirculation zones in a typical micromix combustion flow. The flame obtained by the present micromix combustor concept is anchored, near the trailing edge of the H_2 injector plate, by these two distinct recirculation zones. A shear layer is established between the two recirculation zones because of the offset of the axial position of the H_2 stream relative to the air stream gate, and hence a reaction zone is established along the inter-recirculation shear layer. The structure and the orientation of the flame structure are influenced by this inter-recirculation shear layer, which in turn is defined by the size and the position of these recirculation zones.

If the hydrogen penetration depth is too great or too small, the hydrogen/air mixture enters one of the recirculation zones (inner or outer). Because these zones contain hot gases this increases the residence time of the hot combustion products and thus increases the NOx formation. Hence it is important to ensure that the penetration of hydrogen is within the desired range in which flames are formed in the shear layer between the two recirculation zones.

The Design of Experiments (DOE), Latin Hypercube Sampling (LHS) design technique is used to determine the design sampling points to generate a wide collection of injector geometries. LHS is an advanced form of Monte Carlo sampling method that avoids clustering samples. In LHS, the points are randomly generated in a square grid across the design space but no two design points share the same value, hence covering a wide range of design possibilities. The H_2 orifice diameter, the air gate dimensions, and the H_2/air offset distance and mixing distance are varied as a part of this analysis. The design limits of each of these parameters are shown in Table 1.

Design Parameter	DOE Range
H_2 Offset Distance	0.5 – 5 mm
Mixing Distance	0.5 – 5 mm
Vertical Injector Distance	5 mm
Horizontal Injector Distance	5 mm
H_2 Inlet Diameter	0.3 mm
Air Gate Aspect Ratio	1- 2
Air Gate Height	1 – 2.5 mm
Air Gate Diameter	1 – 2.5 mm

Table 1. Micromix injector design parameters range

The primary design parameters including the H_2 gate dimensions and the air gate dimension directly influence the momentum flux ratio of the JICF and hence the mixing characteristics. The range for these parameters is selected such that the momentum flux ratio varies between 0.85-38. This range is selected based on the various analyses previously carried out by Cranfield [10], which indicated that this range would cover various flow and flame patterns for the specific injector spacing. The spacing is estimated based on the required energy released per unit area for a typical annular combustor of a turbofan engine. The H_2/air mixing distance and the offset distance design limitations are imposed based on the concept of micromix diffusion flame. Further increase in offset distance significantly reduces the effect of air acceleration via air gates. Whereas further increase in mixing distance leads to creation of a pre-mixing zone and the risk of flashback on the injector surface arises.

Several selection criteria were used to down-select the injector designs for rig test. The injector designs need to cover a range of momentum flux ratios, offset distances and mixing distances to ensure that different flame lengths, positions and shapes will be observed. This also ensures that various types of flame interaction will occur, such as: no interaction, interaction between flames sharing same feeding arm and interaction between flames of jets from neighbouring feeding arms.

2. Numerical setup and test conditions

The numerical domain is shown in Figure 4. It consists of two micromix injectors including two air gates and two hydrogen injection orifices connected by one feeding arm with mass flow inlet from both sides of the arm. The air is fed with a mass flow inlet of 3.865g/s upstream of the air gate. Downstream of the injection, in order to represent a very large injector array, the upper and lower sides are set to symmetry and the left and right sides are set to periodic boundaries. The exit of the domain is at 60mm downstream of the hydrogen injection and set to pressure outlet. For all cases in this study the operating pressure is set to 15 bar, the hydrogen and air inlet temperatures are set to 300K and 600K respectively and an equivalence ratio of 0.4 is selected. The parameters of a baseline design are listed in Table 2.

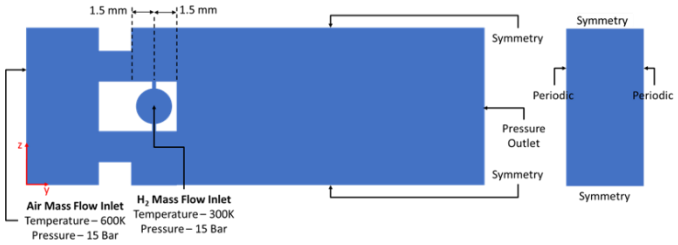

Figure 4. Numerical domain and imposed boundary conditions

Design Parameter	Value
H_2 Offset Distance	1.5 mm
Mixing Distance	1.5 mm
H_2 Inlet Diameter	0.3 mm
Air Gate Aspect Ratio	1.5
Air Gate Exit Area	3.2mm^2
Momentum Flux Ratio	1.95

Table 2. Baseline design key parameters

The mesh size is determined via a grid independence study, to ensure that the computational cost is acceptable without compromising the accuracy. The flame region is refined with a cell size of 0.08mm with 10 prism layers in the vicinity of the wall.; a y+<2 is used for walls within the flame region. Downstream of the estimated recirculation area, the mesh size is kept close to 0.3mm.

Three-dimensional steady RANS analysis is performed for all cases presented in this paper using ANSYS FLUENT (for the studies in Section 3 and 4) and Star-CCM+ (for the study presented in Section 5). The k-omega SST turbulence model is used as the shear stress transport (SST) formulation allowing for integration down to the wall, through the viscous sub layer, resulting in a more accurate near wall treatment [11]. This is vital for designs involving jets in cross flow, ranging from miniaturised mixing characteristics close to the hydrogen jet to the larger eddies in the combustion zones with presence of shear layers and strong recirculation. The fluid is considered as a compressible ideal gas.

A Flamelet Generated Manifold (FGM) with diffusion flamelets is employed for modelling hydrogen combustion and turbulence-chemistry interaction. This model assumes that the chemical reaction process occurs much faster than the than integral time scale of the turbulent flow. If the smallest scale of eddies do not significantly impact on the chemical reactions, the turbulent flame can be considered as a differential set of laminar flames. The chemistry is defined by mixture fraction and progress variable so that the scalars can be pre-tabulated. A Probability Density Function (PDF) is used to mimic the effect of turbulence on chemistry. For hydrogen air mixture, the diffusion feature is modified by varying the PDF Schmidt number from the default value of 0.7 to 0.25, to accommodate the much higher mass diffusivity of hydrogen compared to hydrocarbon fuels. Ideally, the Lewis number should also be decreased for the same reason, however, the FGM assumes a unity Lewis number for flamelet generation [12], it remains one

of the main limitations when this approach is applied. Further justification on the validity of using FGM and relevant model constants for micromix combustion is included in [13]. A 9-species 25-steps mechanism [14] is used for hydrogen reaction. Previous work has proven that it is a good compromise between accuracy and computational cost [10, 15]. The concentration of thermal NOx was calculated using the Zeldovich mechanism implemented in the CFD tools with a post-processing by freezing the flow field [16].

3. Analysis of four down-selected injector designs

Four injector designs were down-selected based on the criteria listed in Section 1. These designs cover a range of momentum flux ratio at reference simulation conditions (i.e. 15bar, 600K air) as well as mixing and offset distance, with an equivalence ratio ϕ of 0.4. The design parameters are listed in Table 3. It is worth noting that the momentum flux ratio varies with the equivalence ratio as the mass flow rate of hydrogen jet changes.

The central plane velocity flow field obtained from simulations of the four designs at the reference condition is presented in Figure 4. It can be seen that for all designs, the inner recirculation vortices can be clearly identified, as described in Section 2. With different combinations of design parameters, the size and position of these recirculation zones vary. For design A (referred as baseline), the size of the inner recirculation zone is the largest amongst the 4 designs, with considerable width and length. Design B has a long but narrower recirculation zone, this is probably related to the fact that the momentum flux ratio is lowest because of the highest air momentum flux. It is therefore more difficult to form reversed flow downstream of the injector

	Air Gate Area	Momentum Flux Ratio	Offset Distance	Mixing Distance
Design A	3.1 mm^2	1.95	1.50mm	1.50mm
Design B	1.9 mm^2	0.74	0.85mm	1.40mm
Design C	5.6 mm^2	6.32	4.75mm	0.86mm
Design D	7.5 mm^2	11.0	2.00mm	2.00mm

Table 3. Design parameters of four down-selected injectors

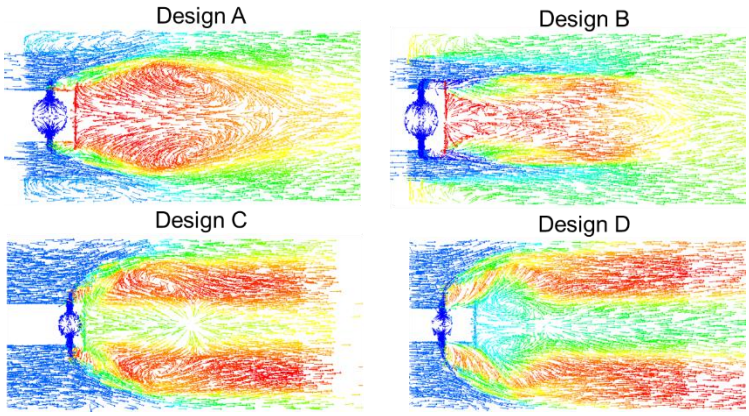

Figure 4. Velocity vector field in the flame region for the four selected designs, coloured by temperature

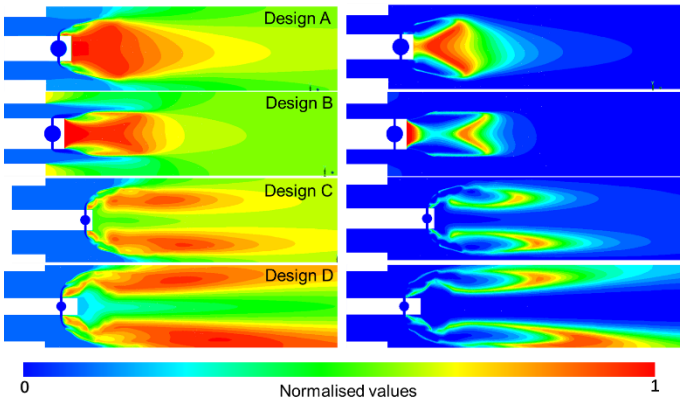

Figure 5. Temperature (left) and OH mass fraction (right) contours of the four down-selected designs

trailing edge. It is interesting to notice that for Design C and D, where the momentum flux ratios are significantly higher than A, the IRZs length is relatively small. As the cross section area of air gates in Design C and D increases from that of A, the higher hydrogen penetration due to the lower air velocity results in a greater distance between the two hydrogen jets and the hydrogen being more vertically (i.e. in z direction) dispersed, hence a more upright positioned shear layer should be expected, with a shorter but wider IRZ. Also, less expansion takes place due to larger area ratio between air agate and downstream, which could result in a smaller IRZ. Finally, compared to A, Design C has a notably longer offset distance but much shorter mixing distance, Design D has both longer offset and mixing distance, the sum of the two distances from the air gate is larger than A for both designs. This implies a greater expansion and dumping effect of air before it reaches the injector plate trailing edge.

The outer recirculation zones are visible at central plane for all four designs. For Design A and B, relatively large dump exists as air exits the gate at relatively high velocity. Compared to IRZ, ORZ size is significantly smaller. For Design C and D, ORZs are less apparent because of less flow expansion.

The temperature and OH mass fraction contours are shown in Figure 5. For all cases the flame and hot combustion zones are vastly different. For Design A, it can be seen that a large amount of the hot combustion product is entrained in the IRZ, the flames are close to the injector plate trailing edge and are shortest amongst the four designs if characterised by the majority of the heat release. The flames from both hydrogen injectors interact immediately downstream of the trailing edge, forming a V shape flame front and the two hot gas streams merge further downstream.

For Design B, the onset of combustion is further downstream. The flame is longer compared to Design A due to lower hydrogen penetration and higher air velocity. Similar to design A, most of the hot products are within in the IRZ. Since the IRZ is narrower, the merging of two hot streams takes place further upstream. The OH distribution suggests that a great portion of the heat release is attached to the injector plate trailing edge, suggesting that excessive wall temperature could occur. The flame interactions occur further downstream than in Design

A due to later combustion onset, a smaller V shape flame front is also presented. For this particular design at reference conditions, there are hot products caught in the ORZ at both corners which could also be a potential concern for the wall temperature.

For Design C, the combustion starts in the vicinity of the hydrogen orifice exit whereas the maximum temperature across the combustion zone is lower. The temperature near the upper and lower injector plate surface downstream of injection is higher than that near the trailing edge surface because of the early onset and high penetration. Hot product is only circulated in a limited region of the IRZ and the two streams show no tendency to merge together. There are no interactions between the flames coming from the same hydrogen feeding channel. It is also worth noting that the flames are longer, which can be explained by the fact that the flame temperature is lower, the heat release is less intense, and there is no interacting hot stream to accelerate the combustion process.

Design D possesses a similar type of flame shape to Design C, with a quick start to combustion and two separate flames. However, there is a temperature rise and an increase in heat release rate further downstream than in D, due to the flames merging with neighbouring flames from upper and lower feeding channels represented by the symmetry planes. Also, there is no hot gas in the IRZ and the trailing edge wall is exposed to significantly cooler flow. Due to the interaction with neighbouring flame from other injectors, the central cooler stream does not merge with the hot gas until the exit of the domain, therefore, hot spots could be expected for this type of flame pattern.

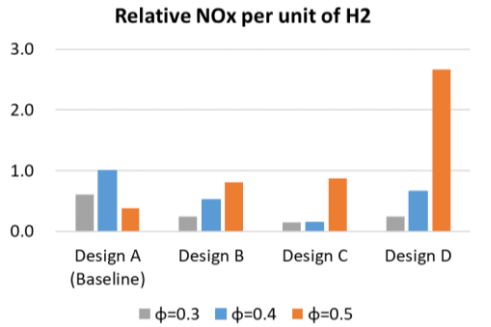

Figure 6. Normalised NOx/H_2 mass flow at various ϕ

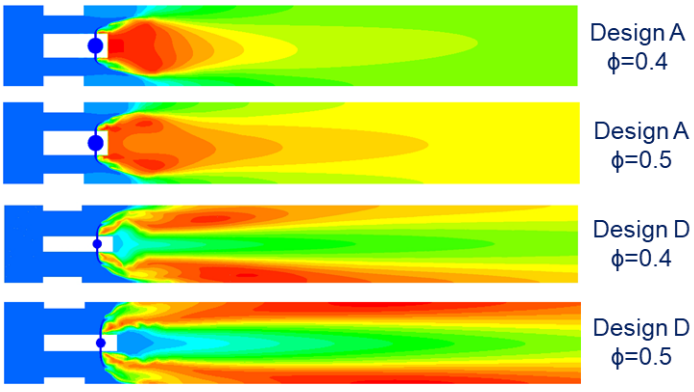

Figure 7. Examples of temperature distribution for Design A and D at various ϕ

NOx emission predictions were carried out for all cases, considering thermal NOx. The values of NOx production per unit of fuel at the outlet, relative to that for Design A with =0.4 are shown in Figure 6. The impact of changing equivalence ratio is also shown.

For an equivalence ratio of 0.4, design C, which has no interaction between flames and a lower combustion temperature, produces lowest NOx. Less NOx is produced in Design B compared Design A to due to the smaller IRZ, which implies both shorter residence time and a smaller amount of hot product trapped. Although no hot product is trapped in IRZ for Design D, NOx is still higher than B and C, because of interaction with neighbouring flames.

By comparing these four designs at a range of equivalence ratios, it can be seen that the equivalence ratio has a significant impact on the results. For the baseline design (Design A), the highest equivalence ratio does not lead to highest NOx per unit of fuel even though the mean temperature is highest. Figure 7 includes the temperature distributions for Design A with ϕ=0.4 and 0.5. It can be seen that for the ϕ=0.5 case the flames are more separated from each other because of the higher momentum flux ratio giving greater hydrogen jet penetration. Therefore, the temperature in the IRZ is lower, thus less NOx is produced. For Design B, increasing ϕ results in an increase in NOx per unit of fuel, which can be explained by the fact that, with the increase in fuel flow rate hence the momentum flux ratio, the size of the IRZ increases and more hot product is involved in this region. It is also expected due to the increase in global equivalence ratio, the flame temperature increases, hence NOx increases. For Design C, the increase of ϕ from 0.3 to 0.4 has insignificant influence on NOx whereas from ϕ=0.4 to 0.5, NOx has increased vastly. Again as J increases with ϕ, the flames starts to interact with neighbouring flames from other injectors from different feeding channel. For Design D NOx per unit of fuel increases dramatically as ϕ increases from 0.4 to 0.5. This results from both the increase in flame temperature (by 30K) due to increase in equivalence ratio and the enhanced flame-flame interaction. As shown in Figure 7, for ϕ=0.5, the interaction with neighbouring flames starts further upstream than the 0.4 case and the unburnt hydrogen jets merge further upstream. The flame and hot product interaction is seen to persist up to the exit of the domain, this indicates a longer flame with increased residence time

4. Effect of various air gate aspect ratios

This analysis aims to investigate the effects of varying air gate aspect ratio on the reactive flow field associated with micromix combustion. The air gate shape is one of the main design parameters because it is responsible for the variation of the aerodynamic features of the reacting flow, particularly the horizontal fuel/air mixing and the size of the recirculation vortices. The D-shaped air gate is with an aspect ratio of 1.5 (i.e. Design A) is used as baseline. The aspect ratio of the air gate is

defined as the ratio between the height and the width of the air gate, as shown in Figure 1. The momentum flux ratio is kept constant by keeping constant the area of the air gate for all the design cases. All other injector design parameters have been kept constant for all cases including the H_2 inlet diameter of 0.3 mm, the H_2/air mixing distance of 1.5 mm and the H_2/air offset distance of 1.5 mm. The inflow boundary conditions i.e. 15 bar operating pressure and equivalence ratio 0.4 is also kept constant. It should be noted that for the subsequent simulations, the computational domain was halved to one injector with symmetric boundary condition to further reduce computational time. This is based on the fact that all the results presented in previous section show good symmetry.

Non-reacting simulations were performed for all design cases to analyse the influence of the varying air feed aspect ratio on the mixing characteristics, without the influence of the combustion process. The vector contour plot of the mole fraction distribution of H_2 across the central plane is presented in Figure 8. It can be seen that the inner recirculation zones, as described in Section 2 are present for all the design cases. However, upon closer examination the size of the IRZ increases and the ORZ decreases as the aspect ratio of the air gate increases. This is because as the air gate aspect ratio increases, so does the height. The increased air gate height reduces the effective distance between the airstream and the injector top wall. This results in reduced strength of the outer recirculation vortex. This reduced strength of the ORZ tends to have very little or no effect on the distribution of the H_2 species. However, it is apparent from Figure 8 that as the aspect ratio of the air gate increases, the position of the IRZ tends to move downwards. This can be attributed to the dumping effect of the air stream. the increase in the height of the flow of the air stream suppresses and pushes the H_2 stream in the downward direction, hence resulting in the downward moment of the inter vortex shear layer and subsequently the inner recirculation vortex.

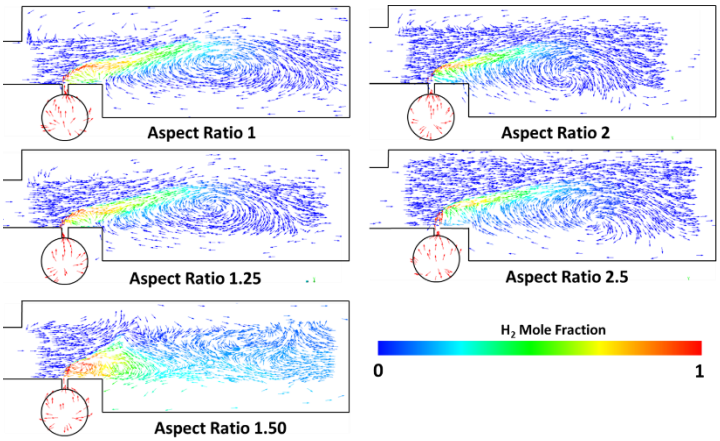

Figure 8. Velocity vector coloured in hydrogen mole fraction

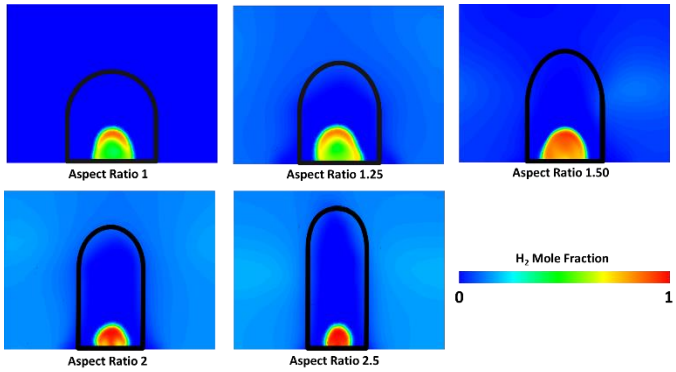

Figure 9. H_2 mole fraction 1mm downstream of injection

The contour plots of the H_2 mole fraction at plane 1 mm downstream of the H_2 injection are presented in Figure 9. As the jet enters the cross-flow its shape begins to change because of the non-uniform pressure field created by the flow around it. The jet is deformed typically into a crescent/horseshoe shape, and the cross-flow creates a pair of vortices behind the jet in much the same way as flow around a cylinder. This formation of the crescent/horseshoe-shaped H_2 jets is visible for some of the design contour plots shown in Figure 9. With an increase in the air gate aspect ratio, two interesting effects can be observed. Firstly, as the aspect ratio increases, the height of the air stream also increases. The increase in the height of the air stream result in a reduction of the H_2 stream penetration (see Figure 9). However, as the aspect ratio increases, the width of the air gate decreases for a constant air gate area, which results in an increased separating distance between the neighbouring H_2/air mixture. This further increases the strength of the recirculation zones present between the mixture and the neighbouring injectors and tends to constrain the diffusion of H_2 to the centre of the domain. This increases the H_2 concentration on at the central plane as shown in Figure 6.

To investigate the mixing characteristics and their influence on NOx formation, an un-mixedness parameter is introduced to quantify mixing characteristics. This parameter is based on the approach reported by Hornsby and Norster [17], who proposed that the degree of mixing could be characterised by a statistical mixture distribution parameter, the mass flow weighted standard deviation of fuel mass fraction, S, defined as follows:

$$S = \sqrt{\frac{\sum(c_i^2 \dot{m}_i)}{\sum \dot{m}_i} - \left(\frac{\sum c_i \dot{m}_i}{\sum \dot{m}_i}\right)^2} \qquad (2)$$

Where c_i is the mass fraction of fuel at cell i and $\dot{m}_i$ is the mass flow through cell i.

When air and fuel are perfectly mixed, this parameter is equal to 0. However, because it is not a normalised parameter, the value of S for perfectly un-mixed cases is dependent on the air-fuel ratio. A normalized version, S_N which equals one for all perfectly un-mixed cases, irrespective of air fuel ratio would facilitate comparison of different cases. This normalised standard deviation is defined as:

$$S_n = \frac{S}{S_0} \qquad (3)$$

Where S_0 is the value of S for fully un-mixed air and fuel. It can be shown that for the fully un-mixed case:

$$S_0 = \sqrt{\left(\frac{1}{AFR+1}\right) - \left(\frac{1}{AFR+1}\right)^2} \qquad (4)$$

Where AFR is the mass-based global air-fuel ratio.

S_n is determined at several planar sections starting from the surface of the injector plate and is shown in Figure 10 for varying aspect ratios. The formation of the shear layer between the two streams in a JICF arrangement results in the formation of two distinct recirculation zones, these recirculation zones further enhance the mixing characteristics. It can also be seen (Figure 10) that as the aspect ratio of the air gate increases S_N increases, indicating that the mixing characteristics have worsened. This is worthy of note as it indicates that despite the momentum flux ratio being constant the shape of the air gate can influence the flow dynamics and thus mixing.

A combusting flow analysis of the same configurations gave the temperature and NOx mass fraction contour plots shown in Figure 11. The NOx concentration at the exit of the domain (relative to the 2.5 aspect ratio case) is marked at the top right of each NOx contour plot. It can be seen that as the aspect ratio of the air gate increases the area of the hot region in the symmetry plane also increases. This may be due to the hot combustion products being trapped in the inner recirculation zone. This resulted in a significant increase in NOx because of the degraded mixing performance and increased residence time of the hot combustion products. It is therefore concluded that a lower aspect ratio yields better NOx emissions because of the factors mentioned above. However, it should be noted that in this case the momentum flux ratio J is relatively low and remains constant. Further investigations could be carried out to investigate whether this conclusion also applies under different conditions producing different flame behaviour.

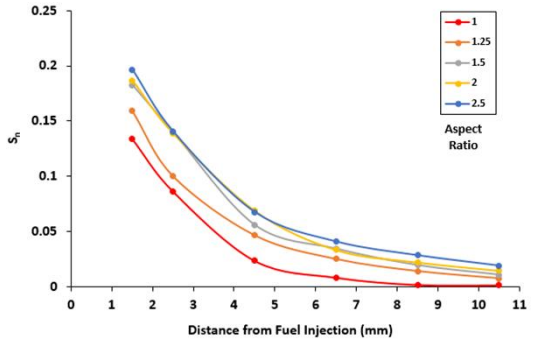

Figure 10. Normalised Standard Deviation of H_2 concentration downstream of hydrogen injection

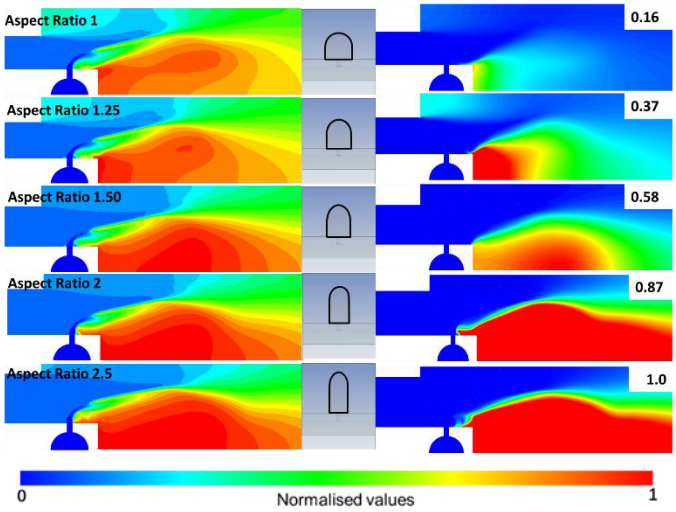

Figure 11. Temperature (left) and NOx mass fraction (right) contours for aspect ratio AR of 1, 1.25, 1.5, 2, 2.5 (normalised by values of AR=2.5 case)

5. Effect of various air gate shapes

This part of the study investigates the effects of the variation of the air gate shape on the fuel-air mixing, flame shape and position and temperature distribution, in order to explore the possibility reducing NOx production further. The boundary conditions and other design parameters remain constant, as does the momentum flux ratio. Six different air gate shapes have been analysed: the baseline D-shape, a circle, a semi-circle, two ellipses with different aspect ratios and a stadium (i.e. a rectangle with semi-circular ends). Unlike the previous work, this part of the study was performed using Star-CCM+.

The temperature distributions at the central plane for all 6 configurations are depicted in Figure 12. The result for an aspect ratio of 1.5 in Figure 11 and Case 1 in Figure 12 are at equivalent conditions. In both cases it can be seen that there is a similar hot region in the IRZ close to the injector plate and aerodynamic and flame behaviour are similar. Differences in the figures are due to presentation differences (i.e. differences in normalisation and colour bar) and modelling differences (there are differences in the approach to FGM flamelet generation in the software). The significance of modelling differences requires further investigation and validation when test data becomes available.

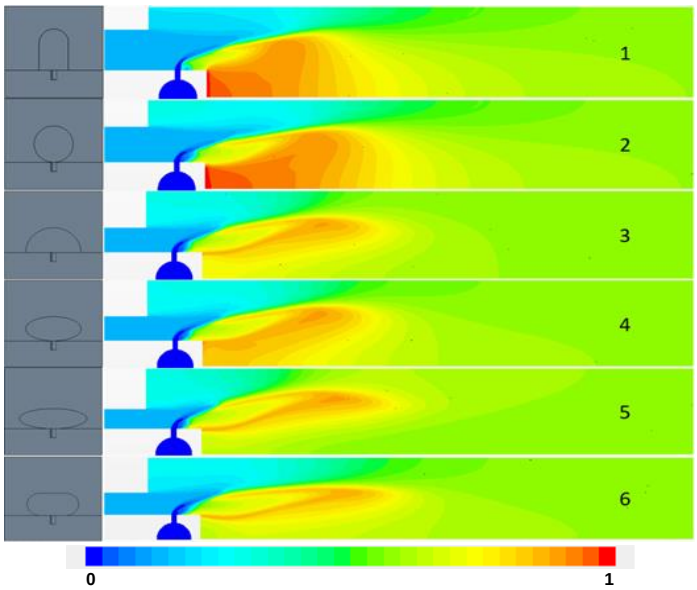

Figure 12. Temperature contours for 6 configurations characterized by different air gate shape at the central plane

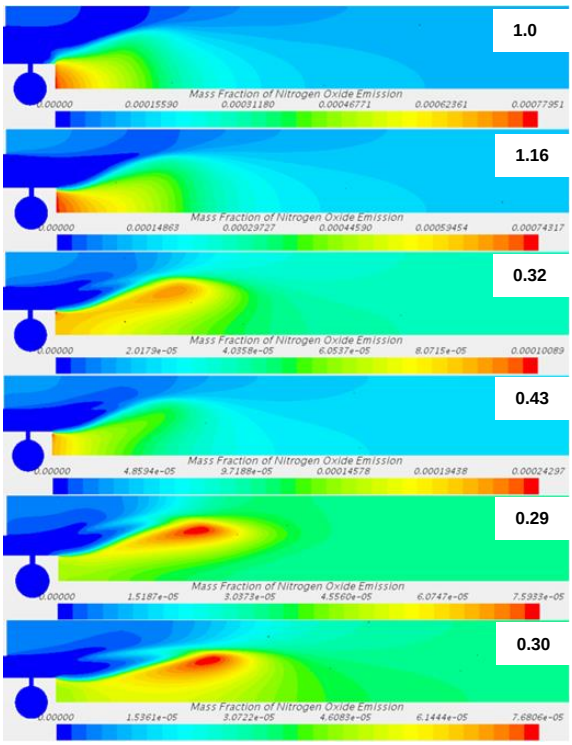

Figure 13. NOx contours configurations 1-6 characterized by different air gate shape at the central plane (Normalised NOx production at outlet included)

Figure 12 shows the temperature distribution for the 6 cases. The first two configurations are characterized by very high temperature in the IRZ, particularly along the injector plate. This is likely to produce high NOx due to the long residence time and high temperature in the IRZ.

However, configurations 3,5 and 6 show a temperature distribution with lower values in the IRZ, and the NOx emissions are expected to be lower. Configuration 4 represents an intermediate case between the two different distributions described.

The contours of mass fraction of NOx (Figure 13) show a NOx distribution consistent with that expected based on the temperature distributions in Figure 12. This confirms the assumption that high temperatures in the IRZ are undesirable and lead to high NOx production. The most desirable distributions are provided by configurations 3, 5 and 6, particularly the last two, in which NOx emissions peak along the shear layer and are considerably lower within the IRZ compared to the first cases.

As with the study detailed in Section 4, non-reacting cases were considered to investigate mixing characteristics independently of the combustion process. The normalised standard deviation evolution is plotted in Figure 14 for the 6 cases characterised by different air gate shapes. Unlike the study in Section 4, there are very similar mixing characteristics for all the configurations according to Sn. While Section 4 indicated that better mixing (i.e. lower Sn) results in lower NOx, this study found large differences in NOx with little difference in mixing quality. This suggests that while the overall fuel-air mixing

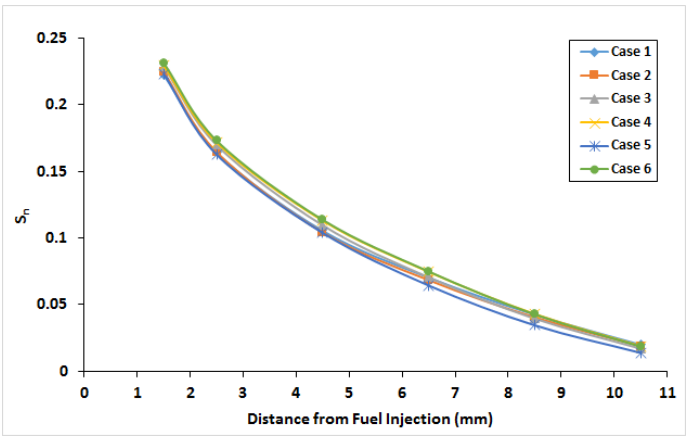

Figure 14. Normalised Standard Deviation of H_2 concentration

quality (as described by Sn) can be an important factor in NOx production, appropriate air and fuel placement (not reflected in Sn) is critical in achieving lowest practicable NOx in hydrogen micromix systems.

For a given jet momentum flux ratio, the distribution of the air within the injection zone and its relationship to the fuel are the key factors in reducing NOx emissions. All the configurations are characterized by the same momentum flux ratio and thus the jet penetrates into the air stream with the same intensity. In this case, an equivalence ratio of 0.4 leads to a momentum flux ratio of around 2.2, which is relatively low. For this momentum flux ratio, a high air gate is not necessary because there is low risk of fuel jet penetration through the incoming air jet into the outer recirculation vortex. However, benefits associated with an increased air gate width are important. Figure 15 illustrates the temperature distributions at the cross-section plane 2.5mm downstream of the fuel injection for configurations 1 and 6. This view shows that, in configuration 1, the air stream flowing from the lowest part of the gate reacts with the hydrogen jet and is recirculated within the inner vortex, causing a significant increase in temperature there. The air flowing from the upper part of the gate does not interact with the fuel stream and remains relatively cool (about 600 K). Whereas in configuration 6 the stadium shape results in the cool air from the upper part of the gate being placed to the sides of the hot combusting fuel jet. In this way, the entrainment between the air and hydrogen streams does not affect the mixing characteristics of the non-combusting jet, but the air placed laterally surrounding the hot gas stream can be entrained, cooling the

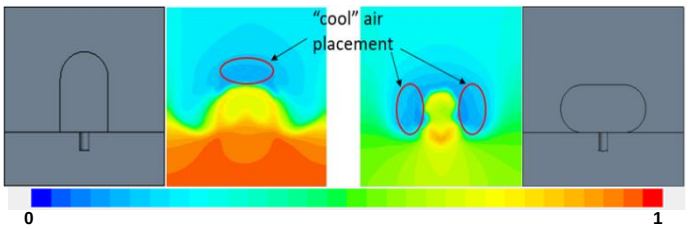

Figure 15. Temperature distributions showing the placement of cool air at the axial section placed at 2.5 mm downstream of the injection hole for the configurations 1 (left) and 6 (right)

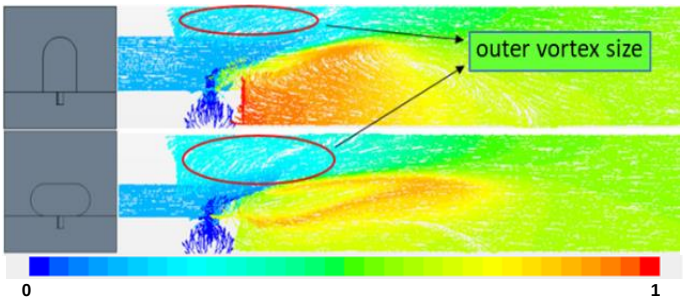

Figure 16. Velocity vectors colored by normalised temperature illustrating the size of the outer vortex for configurations 1 and 6

gases entering the inner recirculation vortex. In addition, a variation of the air gate height has a direct influence on the size of the recirculation vortices, leading to a significant change in the aerodynamics of the reacting flow (Figure 16). A reduction of the air gate height causes the formation of a larger outer vortex and, due to the higher concentration of air in the lowest part, the inner vortex size is significantly reduced. This affects the flame position and shape with the flame now being stabilized within a longer shear layer, which is clearly illustrated in Figure 16.

CONCLUSION

Three numerical studies on the effect hydrogen micromix injector designs have been presented in this paper, showing various configurations which resulted in vastly different flow and flame structures.

The first part of the study demonstrates that the effect of momentum flux ratio is critical to the flame and temperature distribution, hence NOx production in a number of ways:

1. At a fixed spacing, the width and length of the inner recirculation zones are determined by the cross section area of the air gate, which is correlated with air velocity and momentum;
2. The flame position is strongly influenced by hydrogen jet penetration height, both axially and vertically
3. The flame position, together with the recirculation zone size and shape, results in different flame-flame interactions, either between the flames with jets sharing the same feeding arm, or with jet from neighbouring feeding arms.
4. Interaction between the flames with jets sharing the same feeding arm is also accompanied by entrainment of hot products into the IRZ, resulting in a longer residence time, therefore more NOx is produced
5. There are also cases that with intermediate hydrogen penetration, both types of interaction are not strong, leading to a rather isolated flame contained in the shear layer, with significantly lower NOx predicted.

This results in the phenomena that for a constant hydrogen jet diameter, higher global equivalence ratio could lead to lower NOx, if the jet penetration is a “sweet spot” where the flame interaction and hot product recirculation are controlled to a minimum.

The second and third numerical studies both come to the conclusion that despite the momentum flux ratio being kept constant, solely by varying the air gate geometry, the flame shape could be dramatically altered. With a lower aspect ratio, the hydrogen is horizontally more dispersed, the flame length is reduced and less hot product is trapped in IRZ. With flatter air gate shape, a longer flame is generated compared to the baseline configuration, however the temperature distribution is greatly improved with a smaller hot spot and lower peak temperature. The behaviours observed in both studies can be explained by the fact that a horizontally wider air gate shape produces more isolated flames and the hydrogen jet (and thus flame) is more exposed to the lateral cool air. This may result in lower NOx emissions and temperatures close to the injector plate. If the momentum flux ratio is constrained due to engine operating conditions, there is the potential to optimise NOx by varying the air gate geometry, to optimise mixing in the horizontal direction and the utilisation of cool air.

The results presented in this paper will help guide the future design space exploration in conceiving most promising low NOx emissions hydrogen micromix designs. A metric better characterising the hydrogen air mixing than the non-dimensionalised standard deviation should be considered. The main uncertainties in hydrogen combustion modelling mentioned in this paper will be further addressed and improved upon using the data generated from the ongoing experimental work carried out within the ENABLEH2 project.

ACKNOWLEDGEMENTS

The ENABLEH2 Project is receiving funding from the European Union’s Horizon 2020 research and innovation programme under grant agreement Nº 769241.

REFERENCES

[1] Advisory Council for Aeronautics Research in Europe (ACARE). Flightpath 2050, page 28, 2011. ISBN: 978-92-79-19724-6.doi: 10.2777/50266. URL http://www.acare4europe.com/sria/flightpath-2050-goals/protecting-environment-and-energy-supply-0.

[2] European Comission. NEW Aero Engine Core concepts (NEWAC), 2006. URL https://cordis.europa.eu/project/rcn/79961/reporting/en

[3] European Comission. Low Emissions Core-Engine Technologies (LEMCOTEC), 2011. URL https://cordis.europa.eu/project/rcn/100239/factsheet/en

[4] European Comission. Ultra Low emission Technology Innovations for Mid-century Aircraft Turbine Engines (ULTIMATE). 2015. URL http://www.ultimate.aero/

[5] V. Sethi, Enabling Cryogenic Hydrogen-Based CO2-free Air Transport (ENABLEH2), Presentation at 9th EASN Conference, Athens, 2019.

[6] European Comission. ENABLing cryogEnic Hydrogen based CO2 free air transport (ENABLEH2), 2018. URL https://cordis.europa.eu/project/rcn/216008/en

[7] Funke H H W, Boerner S, Keinz J, et al. Experimental and Numerical Characterization of the Dry Low NOx Micromix Hydrogen Combustion Principle at Increased Energy Density for Industrial Hydrogen Gas Turbine Applications[C]//ASME Turbo Expo 2013: Turbine Technical Conference and Exposition. American Society of Mechanical Engineers Digital Collection, 2013.

[8] Funke H H W, Keinz J, Kusterer K, et al. Development and Testing of a Low NOX Micromix Combustion Chamber for an Industrial Gas Turbine[J]. International Journal of Gas Turbine, Propulsion and Power Systems, 2017, 9(1).

[9] Ayed A H, Kusterer K, Funke H H W, et al. CFD based exploration of the dry-low-NOx hydrogen micromix combustion technology at increased energy densities[J]. Propulsion and Power Research, 2017, 6(1): 15-24.

[10] Agarwal P, Sun X, Gauthier P Q, et al. Injector Design Space Exploration for an Ultra-Low NOx Hydrogen Micromix Combustion System[C]//ASME Turbo Expo 2019: Turbomachinery Technical Conference and Exposition. American Society of Mechanical Engineers Digital Collection.

[11] Menter F R. Two-equation eddy-viscosity turbulence models for engineering applications[J]. AIAA journal, 1994, 32(8): 1598-1605.

[12] Van Oijen J A, Donini A, Bastiaans R J M, et al. State-of-the-art in premixed combustion modeling using flamelet generated manifolds[J]. Progress in Energy and Combustion Science, 2016, 57: 30-74. URL http://dx.doi.org/10.1007/s10494-015-9666-5.

[13] López-Juárez M. CFD evaluation of flame characteristics and emission of H2 micromix combustor injectors. Cranfield University. United Kingdom, Cranfield, 2019, 156 pages.

[14] Reaction Design: San Diego, 2015. ANSYS Chemkin Theory Manual 17.0 (15151).

[15] Babazzi G, Gauthier P Q, Agarwal P, et al. NOx Emissions Predictions for a Hydrogen Micromix Combustion System[C]//ASME Turbo Expo 2019: Turbomachinery Technical Conference and Exposition. American Society of Mechanical Engineers Digital Collection.

[16] Gauthier P Q. Comparison of Temperature Fields and Emissions Predictions Using Both an FGM Combustion Model, With Detailed Chemistry, and a Simple Eddy Dissipation Combustion Model With Simple Global Chemistry[C]//ASME Turbo Expo 2017: Turbomachinery Technical Conference and Exposition. American Society of Mechanical Engineers Digital Collection, 2017.

[17] Hornsby C, Norster E R. Application of CFD to DLN Combustion[C]//ASME 1997 International Gas Turbine and Aeroengine Congress and Exhibition. American Society of Mechanical Engineers Digital Collection, 1997.

Numerical investigation into the impact of injector geometrical design parameters on hydrogen micromix combustion characteristics

Sun, Xiaoxiao

2021-01-11

Sun X, Agarwal P, Carbonara F, et al., (2021) Numerical investigation into the impact of injector geometrical design parameters on hydrogen micromix combustion characteristics. In: ASME Turbo Expo 2020, 21-25 September 2020, London, Virtual Event. Paper number GT2020-16084
https://doi.org/10.1115/GT2020-16084